Probing Weak Forces in Granular Media through Nonlinear Dynamic Dilatancy: Clapping Contacts and Polarization Anisotropy

V. Tournat,[1] V. Zaitsev,[2] V. Gusev,[1] V. Nazarov,[2] P. Béquin,[1] and B. Castagnède[1]

[1]*Université du Maine, Avenue Olivier Messiaen, 72085 Le Mans Cedex 09, France*

[2]*Institute of Applied Physics, 46 Uljanova Street, Nizhny Novgorod, 603950, Russia*

(Received 25 April 2003; published 24 February 2004; publisher error corrected 26 February 2004)

Rectification (demodulation) of high-frequency shear acoustic bursts is applied to probe the distribution of contact forces in 3D granular media. Symmetry principles allow for rectification of the shear waves only with their conversion into longitudinal mode. The rectification is due to nonlinear dynamic dilatancy, which is found to follow a quadratic or Hertzian power law in the shear wave amplitude. Evidence is given that a significant portion of weak contact forces is localized below 10^{-2} of the mean force — a range previously inaccessible by experiment. Strong anisotropy of nonlinearity for shear waves with different polarization is observed.

DOI: 10.1103/PhysRevLett.92.085502 PACS numbers: 81.05.Rm, 43.25.+y, 81.70.Cv

Introduction.—By manifesting properties of unusual solids, fluids, or gases under certain conditions, granular media have become the subject of increasing interest to a wide audience of physical scientists [1]. For prediction of the macroscopic mechanical behavior of granular packing the knowledge of the interparticle force distribution is essential. There is a consensus between theory and experiment concerning the abrupt exponential decay in the probability $P(f)$ of finding contacts that carry forces f larger than the average force f_0 [1–7]. However, there is no consensus on the distribution of forces for those weaker than the average: there are predictions for both decreasing [4] and increasing [5–7] $P(f)$ for $f < f_0$. The existing experimental methods [1–4], which include the carbon paper method, the use of the balance to measure normal forces at the bottom of the packings, or visualization methods, have been lacking so far in their range of sensitivity to delineate between theories concerning the distribution of very weak forces ($f \ll f_0$). In reality, all these methods probe effects that increase with interparticle force and, as a result, give measurements in which response of heavily stressed contacts dominates.

Under these circumstances it is highly desirable to develop experimental methods in which the signal from the weak contacts is higher than from the strong ones. To satisfy this requirement it is proposed in this Letter to use nonlinear acoustics (NA) effects, which are known to be selectively sensitive, in contradiction to simple intuition, to the weakest mechanical structural features of the material [8]. In contrast with earlier approaches [1–4], the NA method described here provides information on $P(f)$ in the bulk, but not at the surface, of three-dimensional granular structures in the previously inaccessible range below a few percent of f_0. The experimental method is based on propagation of bursts of high-frequency (HF) acoustic waves to produce demodulation which is recorded to evaluate $P(f)$. In nonlinear acoustics [9,10], the device based on this principle is called the nonlinear parametric antenna (NPA). In the research described here the shear (S) wave based NPA is used for the first time. The excitation of the low-frequency S wave due to the rectification of HF S waves is known to be forbidden by the symmetry principle [11]. The operation of the shear NPA is possible due to dilatancy [12,13], the tendency of granular materials to expand upon shearing providing nonlinear conversion of S into longitudinal (L) waves. The effect of S-wave rectification with conversion into L wave can be used for determining the amplitude law of the dynamic dilatancy. The choice of S waves was additionally motivated by the expectation that the nonlinearity of granular media has anisotropy which might be probed by rotating the polarization of the S wave.

Preliminary arguments.—Here we present instructive arguments elucidating why nonlinear acoustic effects are preferentially sensitive to the presence of the weakest contacts, which hardly manifest themselves in linear sound propagation. The Hertz nonlinearity of the contacts [14] yields, in the simplest case of equal contact loading, the following relationship between macroscopic stress σ and strain ε of the material:

$$\sigma = bn\varepsilon^{3/2}H(\varepsilon). \tag{1}$$

Here the factor b depends on elastic moduli of the grains, n is the average number of the contacts per grain, and the Heaviside function $H(\varepsilon)$ indicates that only compressed ($\sigma, \varepsilon > 0$) contacts contribute to the stress in the material. In real granular materials there are differently loaded contacts [1–7] that contribute to the resultant $\sigma(\varepsilon)$. To illustrate the role of different contacts in linear/nonlinear phenomena let us suppose that the granular material contains only two fractions of contacts which are differently strained. Separating the static (σ_0, ε_0) and oscillatory ($\tilde{\sigma}, \tilde{\varepsilon}$) parts in the total macroscopic stress and strain, and adding the contributions to total stress from both

fractions we get with the use of Eq. (1)

$$\sigma_0 + \tilde{\sigma} = bn_1(\varepsilon_0 + \tilde{\varepsilon})^{3/2}H(\varepsilon_0 + \tilde{\varepsilon}) + bn_2(\mu\varepsilon_0 + \tilde{\varepsilon})^{3/2}H(\mu\varepsilon_0 + \tilde{\varepsilon}). \quad (2)$$

Here n_1 and n_2 are the mean numbers of contacts per grain of two considered fractions. The dimensionless parameter μ in Eq. (2) takes into account that the static prestrain of the two fractions is different while the dynamic strain is the same. The reason for this may be understood from the evaluation of the strain in the straight vertical chains of beads presented for illustration in Fig. 1. If the height h of the chains oscillates near its average value $h = h_0 + \tilde{h}$, then the strain in the chain composed of N beads of a diameter d each is equal to $\varepsilon = (Nd - h_0 - \tilde{h})/Nd$. Let the bead number $N_0 = h_0/d$ correspond to zero strain in the absence of acoustic loading. Counting the number of beads in the ith column relative to this neutral level ($N_i = N_0 + \Delta N_i$, $i = 1, 2$) and taking into account that $\Delta N_i/N_0 \ll 1$ and $|\tilde{h}|/h_0 \ll 1$, the strain in the column can be approximated by $\varepsilon_i \simeq \Delta N_i/N_0 + \tilde{h}/h_0$. Consequently, the dynamic strain component $\tilde{h}/h_0 = \tilde{\varepsilon}$ is the same for grains belonging to different chains because they have the same static height. In contrast, the static strain $\varepsilon_0^{(i)} \equiv \Delta N_i/N_0$ for the two columns presented in Fig. 1 is different since they contain different numbers of grains ($\Delta N_1 \neq \Delta N_2$). Note that the difference in $\varepsilon_0^{(i)}$ for these columns can be very strong even for $\Delta N_i/N_0 \ll 1$. Clearly the above model is a quasi-1D version of what is expected when force chains shield a part of the grains ("spectators") from being strained. However, even in 3D packings (with essential tortuosity of force chains) the dynamic strain in the first approximation is the same at all the contacts.

In Eq. (2) it is assumed that the second fraction is weakly loaded in comparison with the first one ($\mu \ll 1$). In the considered geometry the meaning of μ becomes clear: $\mu = \Delta N_2/\Delta N_1 \ll 1$. Then under the assumption $n_1 \sim n_2$ it follows that it is the first fraction that predominantly carries the static loading and $\varepsilon_0^{(1)} = \Delta N_1/N_0$ approximates the macroscopic strain ε_0. Summation over a unit area of the elastic forces from individual chains yields the macroscopic stress in Eq. (2).

For initially compressed contacts with $\mu > 0$ and $|\tilde{\varepsilon}| \ll \mu\varepsilon_0$, Eq. (2) can be expanded into series in powers $\tilde{\varepsilon}^m$ with expansion coefficients $d^m\tilde{\sigma}(\varepsilon_0)/d\tilde{\varepsilon}^m$ characterizing the linear and nonlinear elastic moduli M_m of the material:

$$M_m \propto \frac{d^m\tilde{\sigma}(\varepsilon_0)}{d\tilde{\varepsilon}^m} \propto bn_1\left(1 + \frac{n_2}{n_1}\mu^{3/2-m}\right)\varepsilon_0^{3/2-m}. \quad (3)$$

Equation (3) indicates that to the linear acoustic signal (term with $m = 1$) the contribution of the weak contacts is proportional to $\mu^{1/2} \ll 1$, and may be negligible for $n_1 \sim n_2$. In contrast to this, to the nonlinearity-induced signals (terms with $m \geq 2$) the contribution of the weak fraction is proportional to $\mu^{3/2-m} \gg 1$, which dominates at sufficiently small static prestrains $\mu \leq 0.1 - 0.01$. Such strains correspond to even smaller forces $f/f_0 \leq 0.03 - 0.001$ which are far beyond the range $f/f_0 \geq 0.1$ commonly accessible by other methods [1–4].

In accordance with Eq. (3), for a small enough primary acoustic wave amplitude $\varepsilon_p \equiv |\tilde{\varepsilon}| < |\mu|\varepsilon_0$ [when the power-series expansion of Eq. (2) is valid] the rectified signal should be quadratic in ε_p: $\langle\tilde{\sigma}\rangle \sim M_2\varepsilon_p^2$. For stronger amplitude $\mu\varepsilon_0 < \varepsilon_p < \varepsilon_0$, the dominating in the nonlinearity second term in Eq. (2) (related to the weak contacts) should be averaged as $\langle(\mu\varepsilon_0 + \tilde{\varepsilon})^{3/2} \times H(\mu\varepsilon_0 + \tilde{\varepsilon})\rangle \simeq \langle(\tilde{\varepsilon})^{3/2}H(\tilde{\varepsilon})\rangle$ producing a rectified signal $\langle\sigma\rangle \sim \varepsilon_p^{3/2}$. Thus, occurrence of the transition $2 \rightarrow 3/2$ in the amplitude behavior of the demodulated signal at certain ε_p should indicate the existence of the contacts with $\mu \sim \varepsilon_p/\varepsilon_0$.

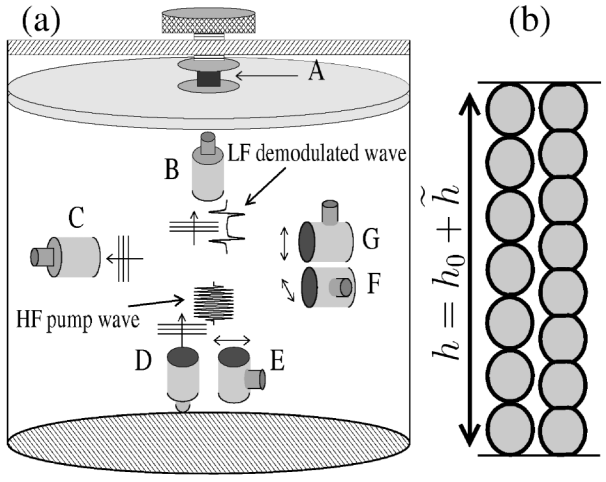

FIG. 1. (a) Diagram of the experiment. A is the force cell; B, C, and D are longitudinal transducers; and E, F, and G are shear transducers. Propagation lengths are 15–20 cm. (b) Two grain chains with essentially different static strains are sketched.

Experimental setup.—We observed the demodulation of intensive L and S elastic waves ("pump") in glass beads 2 ± 0.1 mm in diameter packed in a plastic cylindrical container, 40 cm in diameter and 50 cm in height (Fig. 1). The vertical loading via a rigid plastic cover was controlled by a force cell [static stress and strain ranges were 10–50 kPa and $(1–5) \times 10^{-4}$, respectively]. L and S transducers (respectively, 4 and 3.5 cm in diameter) produced the pump bursts with carrier frequency of 30–80 kHz. The same type L transducers were used for reception. Orientations and polarizations of the transducers are shown in Fig. 1.

Evidence for weak forces localization.—The radiated HF modulated L and S waves were demodulated as a result of contact nonlinearity of the granular medium. The HF pump decayed within a few cm distance, so that only the demodulated low-frequency (LF) signal of ~4–6 kHz characteristic frequency was received. In Fig. 2 the observed dependencies of the LF-signal amplitude on the L- and S-pump amplitudes are shown. The

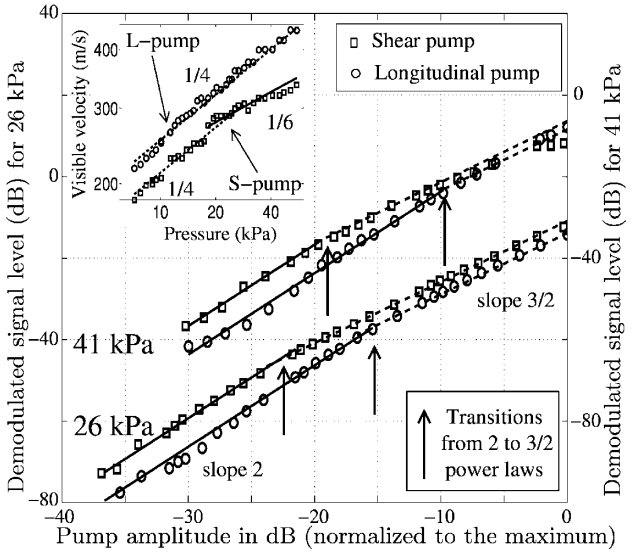

FIG. 2. Demodulated signal amplitude versus pump amplitude (vertical propagation). Inset: pressure dependence of visible (via the time delay) velocities of the demodulated pulses (with slope 1/4 higher than 1/6 expected for equally loaded contacts) indicates gradual activation of weak contacts.

main feature for both L and S pumps in Fig. 2 is the initial quadratic increase in the demodulated signal amplitude with a rather clear transition to the 3/2 law corresponding to the Hertz clapping nonlinearity. Importantly, this transition occurs at an oscillating pump strain ε_p 15–20 dB lower than the mean static strain ε_0, which, as elucidated above, is a signature of weak clapping contacts indicating strong localization of the contact-force distribution $P(f)$ below a few percent of the mean force. For Hertzian contacts where f/f_0 is proportional to $\mu^{3/2}$, the contact-force distribution $P(f)$ can be expressed as a contact-strain distribution $n(\mu)$, or vice versa, through the relation $P(f)df \propto n(\mu)d\mu$. It is often argued [2,3] that the force distribution below the mean value f_0 has a plateau $P(f) = \text{const}$, or it is at least rather flat on a logarithmic scale [5,6]. However, we made a simple computation of the rectified signal $\langle\sigma\rangle$ using in Eq. (2) $n(\mu) = \text{const}$ over the range $0 \le \mu \le 1$, this distribution being equivalent to $P(f) \sim f^{-1/3}$, which is rather close to theoretical prediction [5]. This computation indicates that the demodulated signal at sinusoidal excitation remains nearly perfectly quadratic in ε_p for the whole range of normalized pump-strain amplitude (Fig. 3, lower curve), despite the clapping of weak contacts with $\mu \le \varepsilon_p/\varepsilon_0$. Indeed, since the distribution $n(\mu) = \text{const}$ has no fraction strongly localized at $\mu \ll 1$, the amount of clapping contacts essentially grows with an increase in ε_p. The resultant demodulated signal thus grows stronger than $\varepsilon_p^{3/2}$ and remains nearly proportional to ε_p^2 until $\varepsilon_p/\varepsilon_0 > 1$, at which point practically all contacts in the material begin to clap producing $\langle\sigma\rangle \sim \varepsilon_p^{3/2}$. Therefore the occurrence of the $2 \to 3/2$ transition at a point $\varepsilon_p/\varepsilon_0 \ll 1$ clearly indicates the existence of an important fraction of contacts strongly localized below $\mu = 0.1$. In the clapping regime, it is the total number of clapping contacts with $\mu \ll \varepsilon_p/\varepsilon_0$ that has the important influence on the demodulated signal amplitude. Thus, to simulate the effect it is enough to add to the background constant $n(\mu)$ at $0 \le \mu \le 1$ a weak contact fraction localized in the rectangle $0 \le \mu \le \mu_0 \ll 1$ (in Fig. 3, $\mu_0 = 0.1$ has been chosen). Fine details of $n(\mu)$ at $\mu \ll 1$ are difficult to reconstruct because of the integral character of its manifestation. However, clearly the localization should be rather strong. At the same time, to fit the experimental data in Fig. 3 the boundary of the strongly localized contact-strain distribution should not be too low (otherwise, for example, $\mu_0 = 0.01$ would provide the transition $2 \to 3/2$ located an order of magnitude lower in ε_p than it was in experiment).

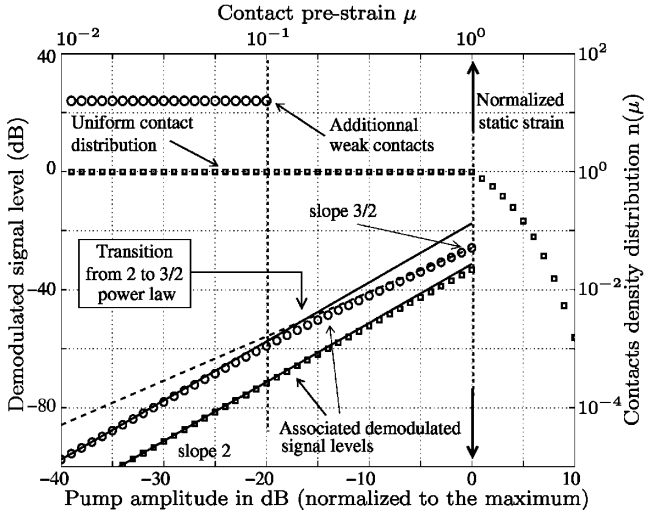

FIG. 3. Demodulated signal amplitude simulated for constant $n(\mu)$ at $0 \le \mu \le 1$ (squares) and in the presence of localized weak fraction (circles) containing 60% of the total contact amount. The latter simulation provides clear transition $2 \to 3/2$ in the slope at $\varepsilon_p \ll \varepsilon_0$.

Nonlinear dilatancy.—Classical Reynolds's dilatancy in the quasistatic deformation of rigid frictionless grains [12] can be qualitatively understood pure kinematically [13] as a combination of grains sliding and rotation past each other. Both the kinematics of incompressible beads [13] and the linearization of the hypoplasticity equations [15] predict the linear volumetric expansion ($\sim|\varepsilon_{\text{shear}}|$) of the granular material under shear. Such an even-type piecewise linear dependence should result in the appearance of a *demodulated longitudinal* signal *linearly* proportional to the S pump amplitude. Concerning the nonlinear S to L wave conversion, the observed demodulated LF pulses clearly had L polarization, and their estimated velocity was almost as high as L wave velocity. The inset of Fig. 4 shows the LF-pulse shapes for two different S pump frequencies. For a lower-frequency pump (that is, longer interaction length with the slower pump S wave) the pulse acquires additional delay, which

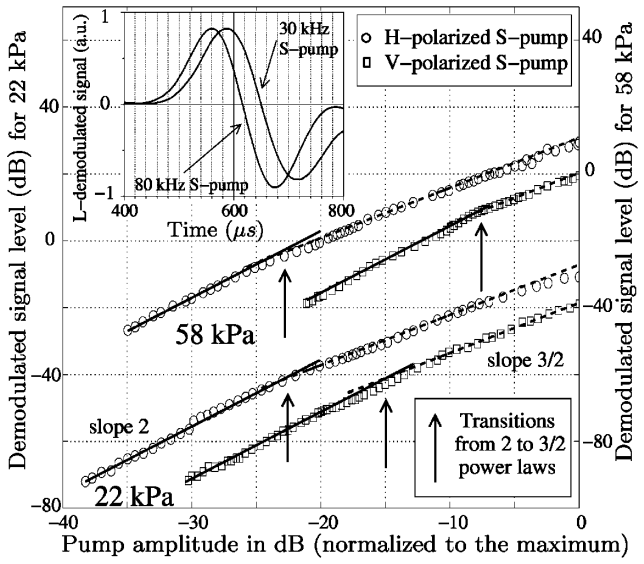

FIG. 4. Demodulated signal level versus S pump amplitude (horizontal paths, H and V polarizations). Inset: demodulated-pulse profiles corresponding to the second derivative of the leading edge of long S pump bursts.

was not observed for different L pump frequencies. However, the observed amplitude character of the S pump demodulation indicates no signs of linear dilatancy [13,15] in the granular material up to $\varepsilon_p \sim \varepsilon_0 \sim (1\text{–}5) \times 10^{-4}$, since the demodulated L pulses exhibit a 2 or 3/2 power in the dependence on the S pump amplitude, thus indicating that the dilatancy is essentially nonlinear. Note that quadratic dynamic dilatancy is predicted for homogeneous solids [11]. Our experimental results demonstrate for the first time an acoustic (dynamic) dilatancy following the power 3/2 of the shear strain amplitude which is the fingerprint of the clapping Hertzian contacts.

Probing contact anisotropy by S waves.—Shear waves can also be used to probe the contact anisotropy and presence of force chains oriented along the applied stress direction through the polarization dependence of the demodulation effect. As noted above, the magnitude of the contact nonlinearity is inversely proportional to the static prestrain [see, e.g., Eq. (3)]; thus, in an anisotropic material different nonlinearity should be expected for different S wave polarizations. Figure 4 shows amplitude dependencies of the demodulated signals from identical S pump sources directed horizontally, but having orthogonal vertical (V) and horizontal (H) polarizations. The plots indicate that, first, the H-polarized pump produced ~10 dB higher-amplitude signals than the V-polarized pump; second, transition to clapping ($2 \rightarrow 3/2$) occurred 7–12 dB lower in amplitude for the H-polarized pump than for the V-polarized pump. Both features indicate a nonlinear parameter several times higher for the H-polarized wave than for the V-polarized wave, which means that the horizontal contacts are, indeed, more weakly loaded than vertical ones by roughly 1 order of magnitude. For a HF shear pump having circular polarization rotating with frequency Ω, this anisotropic dilatancy may result in a demodulated L wave at even harmonics $2k\Omega$, $k = 1, 2, \ldots$.

Conclusions.—The results obtained confirm that NA effects can selectively probe the weak contact portion of the force distribution in granular media despite a rather high background of strong force contacts. In order to explain the signal magnitude and the clear transition $2 \rightarrow 3/2$ in the amplitude dependence of the demodulated wave, it is necessary to assume a large fraction of weak contacts over 60%–70% of the total, which is strongly localized near zero force. For irregular grain shapes, as in dry sand, the localization is even stronger, since the initially quadratic dependence could not be observed at all [10]. The localization extracted from our data is strong in the sense that it is inconsistent with a smooth power law of the form $P(f) \propto f^{-\alpha}$ ($f < f_0$) predicted both for 2D monodisperse granular systems with friction ($\alpha = 0.5$) [6] and 2D polydisperse frictionless systems ($\alpha = 0.3$) [5]. Our inferences agree qualitatively with recent 3D molecular dynamics simulation [7] of monodisperse unloaded packings with friction indicating an abrupt upturn in $P(f)$ at very small values of f ($f \leq 0.1 f_0$), and should stimulate further theoretical modeling.

The study was partially supported by RFBR (Grants No. 02-02-08021-inno and No. 02-02-16237).

[1] H. M. Jaeger, S. R. Nagel, and R. P. Behringer, Rev. Mod. Phys. **68**, 1259 (1996); M. E. Cates, J. P. Wittmer, J.-P. Bouchaud, and P. Claudin, Phys. Rev. Lett. **81**, 1841 (1998).
[2] D. L. Blair *et al.*, Phys. Rev. E **63**, 041304 (2001).
[3] G. Lovoll, K. J. Maloy, and E. G. Flekkoy, Phys. Rev. E **60**, 5872 (1999).
[4] C.-h. Liu *et al.*, Science **269**, 513 (1995).
[5] F. Radjai *et al.*, Phys. Rev. Lett. **77**, 274 (1996).
[6] S. Luding, Phys. Rev. E **55**, 4720 (1997).
[7] L. E. Silbert, G. S. Grest, and J.W. Landry, Phys. Rev. E **66**, 061303 (2002).
[8] I. Yu. Belyaeva and V. Yu. Zaitsev, Acoust. Phys. **43**, 594 (1997); V. Zaitsev, V. Gusev, and B. Castagnède, Phys. Rev. Lett. **89**, 105502 (2002).
[9] B. K. Novikov, O.V. Rudenko, and V. I. Timochenko, *Nonlinear Underwater Acoustics* (ASA, New York, 1987).
[10] V. Y. Zaitsev, A. B. Kolpakov, and V. E. Nazarov, Acoust. Phys. **45**, Pt. I, 235 (1999); **45**, Pt. II, 347 (1999).
[11] L. K. Zarembo and V. A. Krasilnikov, Sov. Phys. Usp. **13**, 778 (1971).
[12] O. Reynolds, Philos. Mag. **20**, 469 (1885).
[13] J. D. Goddard and A. K. Didwania, Q. J. Mech. Appl. Math. **51**, 15 (1998).
[14] K. L. Johnson, *Contact Mechanics* (Cambridge University Press, Cambridge, 1985).
[15] D. Kolymbas, Int. J. Numer. Anal. Methods Geomech. **19**, 415 (1995).